ISSN 8755-6839

SCIENCE OF TSUNAMI HAZARDS

Journal of Tsunami Society International

Volume 38 Number 4 2019

NUMERICAL TSUNAMI MODEL NAMI-DANCE

Andrey Zaytsev [1,2], Andrey Kurkin [1], Efim Pelinovsky[1-4], and Ahmet C. Yalciner [5]

[1] Nizhny Novgorod State Technical University n.a. R.E. Alekseev, Nizhny Novgorod, Russia
[2] Special Research Bureau for Automation of Marine Researches, Yuzhno-Sakhalinsk, Russia
[3] Institute of Applied Physics, Nizhny Novgorod, Russia
[4] National Research University – Higher School of Economics, Moscow, Russia
[5] Middle East Technical University, Department of Civil Engineering, Ankara, Turkey

ABSTRACT

The numerical tsunami model NAMI-DANCE solving the equations of the nonlinear-dispersive theory of long waves is described. It is developed in cooperation of Turkish and Russian specialists and has been used to simulate tsunami characteristics since 2003. The basic model solver simulates the wave propagation with the well-known nonlinear shallow-water equations. The numerical scheme is based on the Leap-Frog method. The long wave dispersion related to the finiteness of water depth is modeled with the help of numerical dispersion by using specific conditions for spatial and temporal steps. The equations are solved in spherical (geographical) coordinates on rotated Earth taking into account nonlinear quadratic friction in the near-bottom layer. The NAMI-DANCE model is adapted to simulate the generation and propagation of tsunamis of various origin from: underwater earthquakes, submarine landslides, and meteo-tsunamis. For the seismic origin tsunami waves, the initial conditions for hydrodynamic equations are found from the Okada solution; the model allows simulating several sources from different fault segments in the earthquake zone. In the case of the meteo-tsunami, the spatial and temporal distribution of the atmospheric pressure is used as external force. The process of generating the landslide origin tsunami waves, is analyzed in the framework of the two-layer model with a lower viscous layer modeling the submarine landslide motion and an upper layer is the water body. The boundary conditions on the open boundaries correspond to the free-wave passage. The run-up process is also computed using the bathymetry and topography at the coastal boundaries. The NAMI-DANCE code has been verified with several benchmarks according to the NTHMP benchmarks. The difficulties of tsunami modelling connected with the lack of accuracy in the bottom bathymetry and the land topography are mentioned. The use of the developed code for the tsunami action analysis on the coasts and constructions is demonstrated.

Key words: *tsunami, underwater earthquake, submarine landslides, meteo-tsunami, shallow-water equations, long wave theory, tsunami action on coasts and constructions*

1. INTRODUCTION

The historical information analysis on the world tsunami shows that, on average, a tsunami happens about once a month, and a catastrophic event approximately happens once a year. Only in 2018, two devastating tsunamis occurred in Indonesia with human casualties. The first of them happened on the Sulawesi Island after a strong earthquake on September 28, when the wave height reached 11 m and more than 2000 people died (Omira et al, 2019). The second was generated by the volcano Anak Krakatau eruption on 22 December 2018, which led to the wave up to 85 m high, which killed about a five hundred people; it was predicted in (Giachetti et al, 2012). Especially, we note the landslide origin tsunami that happened in Russia in December 2018 on the Bureya River with the wave up to 90 m high, fortunately it occurred in uninhabited places (Makhinov et al, 2019). Finally, the meteo-tsunami with the height of 1.5 m is worth mentioning, which occurred in Spain on July 16 (Science Global News, 2018). Even this simple event list for 2018 shows the whole variety of tsunami generation mechanisms.

There is a huge amount of literature describing tsunami modelling with the use of various numerical models. Here we describe our numerical model NAMI-DANCE that solves the equations of nonlinear-dispersive theory of long waves. We have been working with this model since 2003, and have applied it for modeling many historical and prognostic tsunami events.

2. NONLINEAR SHALLOW-WATER EQUATIONS SOLVED BY NAMI-DANCE

The catastrophic tsunami is often global in nature and, originating in one place, can remain very destructive at a distance of tens of thousands of kilometers from the source. Therefore, there is a need to solve the shallow water equations on the real Earth, taking into account its rotation, variable bottom bathymetry and the rugged coastline, as well as the friction influence in the turbulent bottom layer. Basic equations are those well-known nonlinear shallow water equations written on spherical coordinates with respect to flow discharges

$$\frac{\partial M}{\partial t}+\frac{1}{R\cos\theta}\frac{\partial}{\partial\lambda}\left(\frac{M^2}{D}\right)+\frac{1}{R\cos\theta}\frac{\partial}{\partial\theta}\left(\frac{MN\cos\theta}{D}\right)+ +\frac{gD}{R\cos\theta}\frac{\partial\eta}{\partial\lambda}+\frac{gn^2}{D^{7/3}}M\sqrt{M^2+N^2}=fN, \tag{1}$$

$$\frac{\partial N}{\partial t}+\frac{1}{R\cos\theta}\frac{\partial}{\partial\lambda}\left(\frac{MN}{D}\right)+\frac{1}{R\cos\theta}\frac{\partial}{\partial\theta}\left(\frac{N^2\cos\theta}{D}\right)+ +\frac{gD}{R}\frac{\partial\eta}{\partial\theta}+\frac{gn^2}{D^{7/3}}N\sqrt{M^2+N^2}=-fM, \tag{2}$$

$$\frac{\partial\eta}{\partial t}+\frac{1}{R\cos\theta}\left[\frac{\partial M}{\partial\lambda}+\frac{\partial}{\partial\theta}\left(N\cos\theta\right)\right]=0, \tag{3}$$

where η is the water surface displacement, t is the time, M and N are the components of the water flow (discharge fluxes) along the longitude λ and the latitude θ on the rotating Earth, $D = h(x, y) + \eta$ is the

total basin depth, $h(x, y)$ is the unperturbed water depth (defined by bathymetric charts), g is the gravity acceleration, f is the Coriolis parameter ($f = 2\Omega \sin\theta$) and Ω is the Earth rotation frequency (the rotation period is 24 hours), R is the Earth radius. In spherical coordinates, the system of equations (1) – (3) is hyperbolic, so it is important to use the fast numerical algorithms.

In practice, it is necessary to take into account the energy dissipation in the bottom turbulent layer in the near-shore zone. The simplest model here is the parametrization of the bottom friction by a quadratic formula (the last terms in the left side of Eqs. (1) – (3)) with a bottom roughness coefficient – n (the so-called Manning formula). This parameterization is widely used in river hydraulics, where special laboratory experiments were carried out, and roughness coefficients were determined for various soil types. Tsunami waves are not stationary hydraulic flows, but their period is large enough for the quasi-static Manning formula to be used. In calculations, as a rule, the constant value $n = 0.015$ m^{-1}s is used, which is the natural bottom characteristic (sand, small pebbles). It should be noted that in the problems of the wave run-up taking into account real buildings, a variable value of the roughness coefficient is now used (see, e.g. (Choi et al, 2012)), it is important for detailed zonation of the coastal flooding by tsunami waves.

The main advantage of the 'spherical' system (1) – (3) is that it is tied to geographical coordinates, which makes it easy to locate the computation results on the ground. In addition, the bathymetry is available in an electronic form and also in the marine charts in geographical coordinates, so that, in contrast, there is a problem of converting bathymetry to a "flat" Earth. The system of shallow water equations should be supplemented by boundary and initial conditions. At the sea boundaries of the computational regions (for example, in straits), the condition of free wave passage through open boundaries is set, which is exact in the framework of the linear theory of shallow water without taking into account the Earth rotation and the simplest geometry of the maritime border

$$\frac{\partial \eta}{\partial t} + \sqrt{gh}\frac{\partial \eta}{\partial n} = 0 \quad , \tag{4}$$

where the derivative $\partial\eta/\partial n$ is calculated normally to the outer boundary of the computational domain. This condition allows us to carry out computations in a limited area, however, we should understand, that in reality any water basin is variable in depth, and the wave coming out from the computation region can return to it after the reflection in the outer basin. This circumstance imposes restrictions on the wave computation time in the basin (which, unfortunately, is not often paid due attention to), therefore, the maritime border should be moved as far as possible.

The shoreline is generally mobile and moves along with the wave climbing the beach. This point is also singular for shallow water equations (the hyperbolicity of the water wave equations is violated in it), moreover, the dissipative term coefficient becomes infinite. The natural boundary condition of the moving shoreline is

$$D(\lambda, \theta, t) = h(\lambda, \theta) + \eta(\lambda, \theta, t) = 0 \quad , \tag{5}$$

that allows studying the wave run-up on the beach and calculating the characteristics of the coastal flooding caused by dangerous sea waves. To calculate the tsunami wave run-up in real water areas, it is

necessary to have a very good seabed bathymetry and topography. The effect of the quality of the bathymetry data on the accuracy of tsunami computations is analyzed in (Kulikov et al, 2016). It is shown that modern digital bathymetry maps, for example, GEBCO, do not provide the adequate reproduction of the bottom topography in numerical models of the wave propagation, so it can lead to significant errors in estimating the maximum tsunami run-up on the coast. In the subsequent work (Ivanova et al, 2017), this effect was demonstrated by the simulation example of the 2006 and 2007 Simushir tsunamis in the central part of the Kuril Islands. It is shown that computations performed on grids with a resolution of 30 arc seconds provide only a qualitative estimate of the distribution of tsunami heights along the coast. At the same time, a quantitative agreement between the simulation results and the observational data can be obtained only for grids with a spatial resolution of at least 10 arc seconds. For instance, the resolution in 3 m is used for the created inundation map of Turkey (Dilmen et al, 2015, Tufekci et al., 2018).

If cliffs are located on the shore that extends almost vertically into the water, the natural boundary condition is the full reflection one

$$\frac{\partial \eta}{\partial n} = 0 \quad \text{or} \quad u_n = 0, \tag{6}$$

here n is the normal to the coastline. The artificial vertical wall is often used at a depth of 5 - 20 m (at the last sea points of the computational grid), on which the boundary condition is (6). This makes it possible to exclude the run-up zone, which is rather laborious in numerical computations (a very fine grid). To determine the run-up characteristics, the computed displacement distribution along the artificial vertical wall is matched with the analytical 1D solution (Choi et al, 2011).

The system of shallow water equations described above is implemented in many numerical models. We chose the international code TUNAMI, described in (Goto et al, 1997) as the original numerical code. It is still widely used in different countries. The numerical scheme is based on finite differences of the "leap-frog" type. Due to the hyperbolicity of the shallow water equations, the time step is chosen from the Courant condition for the stability of the numerical scheme

$$\frac{R\Delta\lambda}{\Delta t}, \frac{R\ \theta}{t\ \Delta} \geq \Delta \sqrt{g h_{\max}}, \tag{7}$$

where $\Delta\lambda$ and $\Delta\theta$ are the steps of the computational grid along the longitude and the latitude; Δt is the time step; h_{max} is the maximum basin depth. The TUNAMI code was improved by our team, in particular, the program was rewritten in C++ (it is a more advanced language compared to Fortran, in which the original TUNAMI program was written) and both the MPI (Message Passing Interface) parallel programming methods and the Open Multi-Processing were used, which significantly reduced the counting time. A new program interface was developed, (Fig. 1) which allows us not only to compute tsunami waves, but also to process the received data. In particular, it is possible to plot spatial distributions of the water level displacement at different time moments, the wave field maxima and minima (which, for simplicity, we call positive and negative amplitudes) and the wave heights along the coast. We called this code NAMI-DANCE, its documentation can be found in (http://namidance.ce.metu.edu.tr/pdf/NAMIDANCE-version-5-9-manual.pdf; http://skbsami.ru/name-dance; http://lmnad.nntu.ru/ru/projects /namidance/). This numerical model is registered in Russia (the

certificate of the state registration of computer codes No. 2014611028 of January 22, 2014) and copyright held in Turkey.

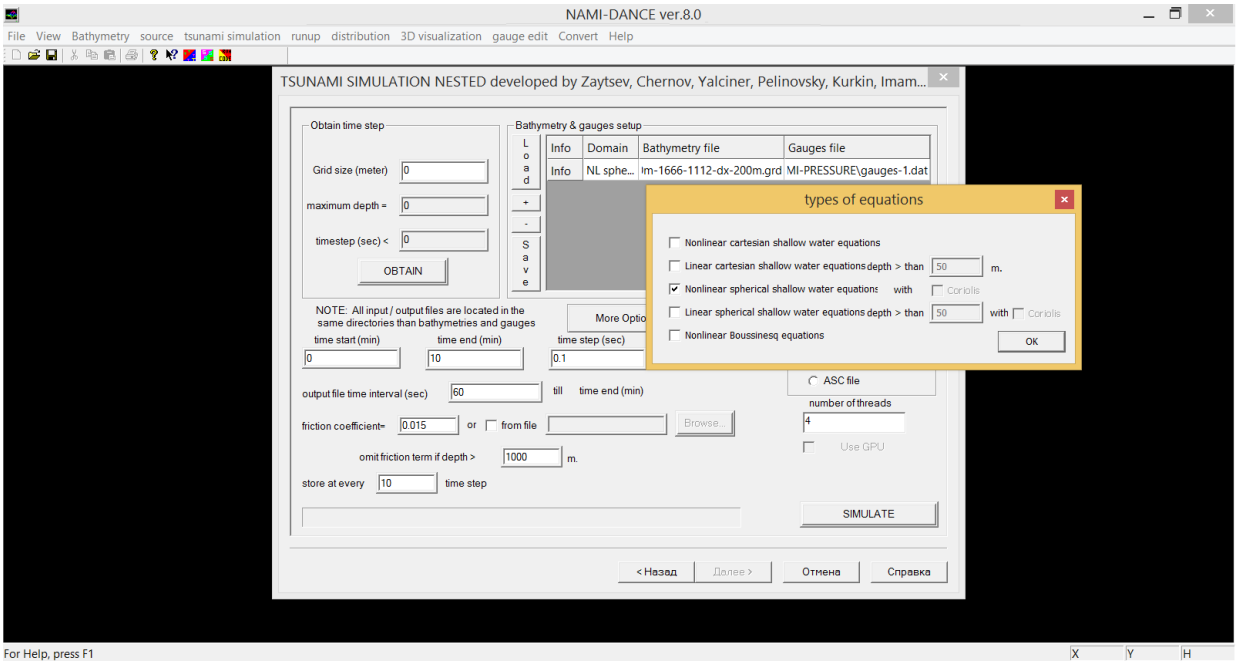

Figure. 1. The interface of the tsunami numerical code NAMI-DANCE.

3. NONLINEAR DISPERSIVE MODEL OF LONG WAVES IMPLEMENTED IN NAMI-DANCE

It is known that for relatively weak earthquakes or landslide tsunamis, the characteristic tsunami wavelength is comparable with the depth of the basin. In this case, the shallow water approximation is insufficient, therefore, it is necessary to use the dispersive long wave model. The same thing may be important for the strongest tsunamis too, if the tsunami source is highly anisotropic. So, the source of the 2004 Indonesian tsunami extended for almost 1000 km along the meridian and about 50 km along the longitude. Consequently, the wavelength varies roughly from 50 km to 1000 km, and in its lower limit it reaches the ocean depth, especially at large distances. The discussion of the dispersion importance for tsunami waves can be found in (Mirchina and Pelinovsky, 1982; Pelinovsky, 2007; Glimsdal et al, 2013; Nosov, 2017).

Nonlinear dispersion long-wave models (the so-called Boussinesq systems) have been already widely used for a long time. Probably, the first of these is the Peregrine system, which is valid for weak nonlinearity and dispersion (Peregrine, 1967). Then a strongly nonlinear weakly dispersive model appears, and here we give some references (Madsen et al, 2003; Pelinovsky, 2007; Kirby et al, 2013; Fedotova et al, 2015; Shokin et al, 2015; Khakimzyanov et al, 2018). Some of them are implemented in the popular open-access codes FUNWAVE (Kirby et al, 1998) and COOLWAVE (Cheung et al, 2003), used to simulate tsunamis and storm surges. However, to implement numerical algorithms to solve the nonlinear dispersion theory equations we need smaller steps in space and time to calculate high-order derivatives. As a result, the computation time increases sharply and numerical errors are accumulated in the computation process over a long distance. It can be indicated, for example, that most of the

numerical schemes of nonlinear dispersion Boussinesq type equations turn out to be unstable (Lovholt and Pedersen, 2009). Another difficulty is the lack of bathymetric maps with a detailed resolution, and their interpolation to small scales is not accurate.

Some other ways of dispersion generalization of shallow water equations that are not related to the introduction of explicitly high derivatives are suggested in (Yoon, 2002; Yoon et al, 2007). This approach is based on the use of numerical dispersion instead of the physical one. The main idea of the method is to change the numerical scheme of finite differences, discretizing the shallow water equations, for the value of the numerical error to lead to the water wave dispersion, as if the dispersion theory equations were strictly solved. It can be demonstrated on the example of one-dimensional Boussinesq equation, to which, in the simplest case, the dispersion long wave theory equations are reduced

$$\frac{\partial^2 \eta}{\partial t^2} - c_0^2 \frac{\partial^2 \eta}{\partial x^2} - \frac{c_0^2 h^2}{3} \frac{\partial^4 \eta}{\partial x^4} = 0 \quad , \tag{8}$$

where $c_0 = \sqrt{gh}$ is the long wave velocity. If we now consider the wave equation (without the last term in (8)), solve it numerically by using the "leap-frog" method as it is done with the initial system of shallow water equations, we will get a different analogue of the wave equation. If we expand all the differences in a Taylor series and restrict them by the first few terms, the differential equation can be obtained again

$$\frac{\partial^2 \eta}{\partial t^2} - c_0^2 \frac{\partial^2 \eta}{\partial x^2} - c_0^2 \frac{(\Delta x)^2}{12} \left(1 - c_r^2\right) \frac{\partial^4 \eta}{\partial x^4} = 0 \quad , \tag{9}$$

where the last term appears, $c_r = c_0 \Delta t / \Delta x$ is the known Courant number, Δt and Δx are the temporal and spatial steps of the numerical scheme. It is important to note that the "leap-frog" scheme makes it possible to exclude the appearance of the third derivative in (9), which would lead to either energy dissipation or instability of the numerical scheme (this is where the requirement to the smallness of the Courant number is followed). However, it is not possible to exclude the terms of the fourth derivative, describing the wave dispersion. Comparing equations (8) and (9) now, we obtain their identity if the step size is chosen equal to

$$\Delta x = 2h / \sqrt{1 - c_r^2} \quad \text{or} \quad \Delta x = \sqrt{4h^2 + gh(\ t)^2 \Delta} \quad , \tag{10}$$

which allows one to connect spatial and temporal steps between each other. This idea is also valid for a variable (but gradual variable) basin depth; in this case, it is necessary to use variable grids (Yoon, 2002). Technically, in (Yoon, 2002) it was proposed to use a constant time step value. As a result, there is no freedom in choosing the spatial grid step because of (10). At variable depths, the spatial grid can be very inhomogeneous, and, therefore, not always convenient for computations. We suggested changing the time step, making the spatial grid more homogeneous. This strategy was implemented in NAMI-DANCE, what allowed us to significantly increase the efficiency of using the numerical dispersion. The description of the scheme is given in (Kian et al, 2018).

We would like to mention that both versions of NAMI-DANCE (with/without dispersion) demonstrated good accuracy on various benchmarks (Velioglu et al, 2016; Lynett et al, 2017; Sogut and Yalciner, 2019).

4. TSUNAMI GENERATION BY EARTHQUAKES

In the case of the tsunami wave generation caused by underwater earthquakes, the seismic process in the source ends quickly enough, and the wave does not have time to leave the source. In this case, the seabed movements can be considered instantaneous, causing the same instantaneous water surface displacement. Then, the wave generation process is reduced to the setting of the initial conditions

$$\eta(\lambda,\theta,t=0)=\eta_0(\lambda,\theta), \qquad M(\lambda,\theta,t=0)=N(\lambda,\theta,t=0)=0. \tag{11}$$

Some time ago, the information about the earthquake was very fragmentary (the coordinates of the earthquake and its magnitude were more or less given), so the initial conditions were determined through empirical formulas (see, for example, (Wells and Coppersmith, 1994; Pelinovsky, 1996)). Now the information is more complete (literally a few minutes after the earthquake) and includes the rupture plane position, the dislocation magnitude, etc. The characteristic parameters of the earthquake source, currently determined quite well, are shown in Fig. 2. They are the fault depth, the length (L) and the width (W) of the fault, the displacement (D), the angle between the meridian and the fault line (Strike angle, θ), the plate slope (Dip angle, δ), the shear angle of the plate (Slip angle, λ). Consequently, it is possible to perform a more complete calculation of residual displacements in the source, based on the theory of half-space elasticity; the corresponding formulas are given in a number of works. In most of our calculations, we use the formulas given in the paper (Okada, 1985) allowing us to determine the function $\eta_0(\lambda, \theta)$ in (8) from the above earthquake characteristics (this approach is now generally accepted). Okada's analytical formulas are very cumbersome (they occupy several pages), by now they have been computerized, therefore, the calculation of the initial water surface displacements can be fulfilled almost instantly.

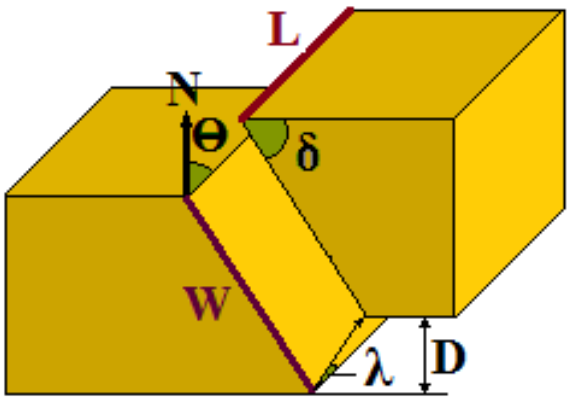

Figure 2. The earthquake parameters

During the strongest earthquakes with magnitudes of the order of 9, the source rupture occurs not instantly, but within several minutes and even tens of minutes. These times are comparable to the characteristic period of tsunami waves, so it is necessary to solve the shallow water equations with the

right-hand side. In theoretical aspect, this problem is discussed, for example, in books (Pelinovsky, 1996; Levin and Nosov, 2009). In practice, however, the extended process of tsunami wave excitation is replaced by several ones, setting instantaneous movements in different time moments and in different points (obtained from the seismic data). The obtained solutions in the open part of the sea are added linearly, and then the general tsunami wave propagation process is analyzed. This procedure is implemented in the NAMI-DANCE model. There are other models used to describe the processes that occur under the influence of the earthquake, for example, a keyboard model developed in (Lobkovsky et al, 2006).

To conclude this section, we list several recently published articles where the NAMI-DANCE model has been used to compute real tsunamis and prognostic inundation maps (Dilmen et al, 2015; Aytore et al, 2016; Zaytsev et al, 2017; Kostenko et al, 2018; Tufekci et al, 2018).

5. TSUNAMI GENERATION BY UNDERWATER LANDSLIDES

According to the statistics, about 85% of tsunami waves are generated by underwater earthquakes, and only a small part is generated by landslides or rockfalls. Landslides often arise as a result of earthquakes, even weak ones, and they can already cause noticeable tsunamis. Such landslides were observed after the most famous catastrophic tsunamis of the seismic origin in recent years, including the last tsunami in Indonesia in 2018, which was mentioned in the Introduction (Sassa and Takagawa, 2019). The viewpoint that tsunamis are caused mainly by landslides and not directly by bottom movements, is rather popular (Yalciner et al, 2003).

In many cases, devastating landslides are produced by local processes in the absence of seismic events. Large amplitude waves associated with landslides were observed in Alaska, Japan and many of the fiords of Norway. Thus, the descent of the 300 million cubic meters avalanche to Lituya Bay (Alaska, July 10, 1958) led to the 60m high tsunami formation, the maximum run-up in the bay itself reached the record value of 524 m. It has already been said about the 40m high tsunami in the Bureya river valley in Russia in 2018. Even earlier, on September 1, 2017 in Baksan in the Caucasus (Russia), a landslide coming down into the river, had generated a wave of 1 m in height (one person died). A tsunami landslide often leads to catastrophic consequences, therefore, the problem of landslide generated waves is of great practical interest.

The numerical simulation of tsunami generation by underwater landslides is a difficult problem, and a number of models have been developed which depend on the rheology of the landslide material; they are discussed in (Imamura and Imteaz, 1995; Pelinovsky and Poplavsky, 1997; Kulikov et al, 1998; Garagash et al, 2003; Pudasaini and Hutter, 2006; Beisel et al, 2010). One of these “shallow-water” models called a two-layer model developed in (Imamura and Imteaz, 1995) is implemented in the NAMI-DANCE code. In the framework of this model, a landslide is assumed to be viscous-liquid and the problem geometry is presented in Fig. 3. The basic equations of the two-layer model have the following form (in Cartesian variables, excluding the Earth rotation)

$$\frac{\partial M_1}{\partial t}+\frac{\partial}{\partial x}\left(\frac{M_1^2}{D_1}\right)+\frac{\partial}{\partial y}\left(\frac{M_1N_1}{D_1}\right)+gD_1\frac{\partial \eta_1}{\partial x}+\frac{gm_1^2}{2D_1^{7/3}}M_1\sqrt{M_1^2+N_1^2}=0 \quad , \tag{12}$$

$$\frac{\partial N_1}{\partial t}+\frac{\partial}{\partial y}\left(\frac{N_1^2}{D_1}\right)+\frac{\partial}{\partial x}\left(\frac{M_1N_1}{D_1}\right)+gD_1\frac{\partial \eta_1}{\partial y}+\frac{gm_1^2}{2D_1^{7/3}}M_1\sqrt{M_1^2+N_1^2}=0 \quad , \tag{13}$$

$$\frac{\partial(\eta_1-\eta_2)}{\partial t}+\frac{\partial M_1}{\partial x}+\frac{\partial N_1}{\partial y}=0 \quad , \tag{14}$$

$$\frac{\partial \eta_2}{\partial t}+\frac{\partial M_2}{\partial x}+\frac{\partial N_2}{\partial y}-\beta\left(\frac{\partial^2\eta_2}{\partial x^2}+\frac{\partial^2\eta_2}{\partial y^2}\right)=0 \quad , \tag{15}$$

$$\frac{\partial M_2}{\partial t}+\frac{\partial}{\partial x}\left(\frac{M_2^2}{D_2}\right)+\frac{\partial}{\partial y}\left(\frac{M_2N_2}{D_2}\right)+gD_2\left[\frac{\rho_1}{\rho_2}\frac{\partial}{\partial x}(\eta_1+h_1-\eta_2)+\frac{\partial}{\partial x}(\eta_2-h_1)\right]+$$
$$+\frac{gm_2^2}{2D_2^{7/3}}M_2\sqrt{M_2^2+N_2^2}=0, \tag{16}$$

$$\frac{\partial N_2}{\partial t}+\frac{\partial}{\partial y}\left(\frac{N_2^2}{D_2}\right)+\frac{\partial}{\partial x}\left(\frac{M_2N_2}{D_2}\right)+gD_2\left[\frac{\rho_1}{\rho_2}\frac{\partial}{\partial y}(\eta_1+h_1-\eta_2)+\frac{\partial}{\partial y}(\eta_2-h_1)\right]+$$
$$+\frac{gm_2^2}{2D_2^{7/3}}N_2\sqrt{M_2^2+N_2^2}=0, \tag{17}$$

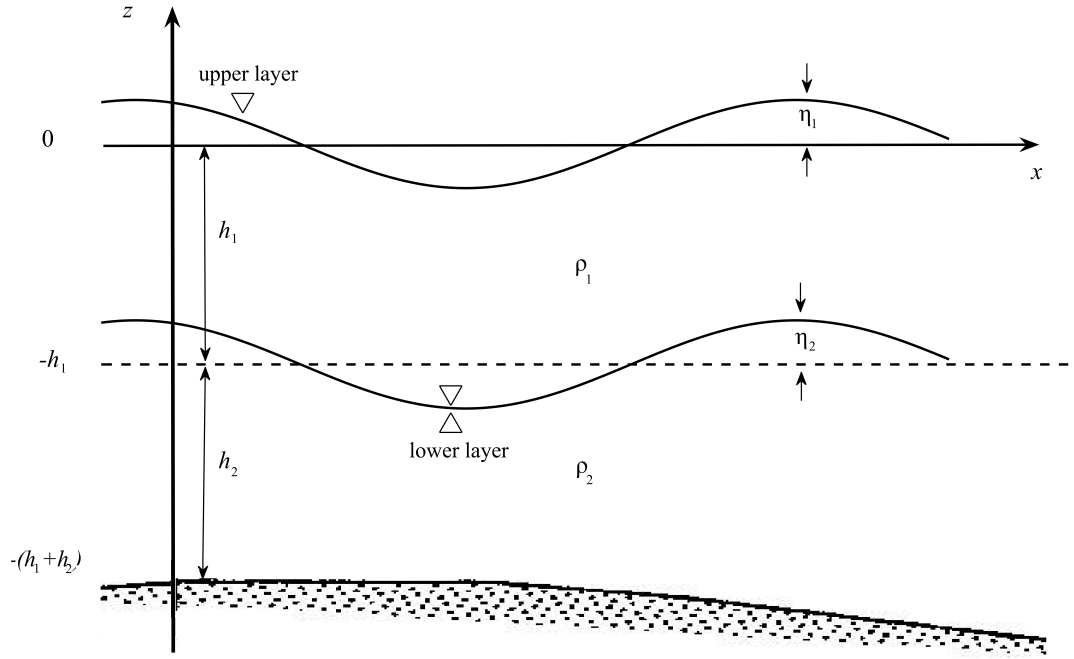

Figure 3. The problem geometry: upper and lower layers correspond to water and landslide, respectively,

where η_1 is the water surface displacement; η_2 is the landslide height; M_1 and N_1 are the water flows along the x and y axes; $D_1 = h_1 + \eta_1$ is the total water depth and h_1 is the undisturbed water depth; M_2 and N_2 are the landslide mass flows along x and y; $D_2 = h_2 + \eta_2$ is the total landslide thickness and h_2 is the undisturbed landslide thickness; m_1 and m_2 are the roughness coefficients of the landslide surface ("liquid" bottom) and solid bottom, respectively, ρ_1 is the water density and ρ_2 is the landslide material density; β is the turbulent viscosity coefficient. It should be immediately noted that the landslide viscosity is taken into account phenomenologically only in one equation (15), providing the landslide spread and its surface smoothness. The vertical structure of the landslide flow is assumed to be uniform in the cross section as in the Savage – Hutter model (Pudasaini and Hutter, 2006). The applicability of such approximations is described in (Imamura and Imteaz, 1995).

The initial conditions determine the landslide location

$$\eta_2(x, y, t = 0) = \eta_0(x, y), \quad M_2 = 0, \quad N_2 = 0, \tag{18}$$

the water surface remains unperturbed (zero initial conditions for η_1, M_1 and N_1). As a result, it is possible to compute the landslide motion and the waves caused by its movement.

Considering the fact that the wavelength of landslide tsunamis is usually much less than those caused by the earthquake, accounting for dispersion effects seems important. That is why we have improved the numerical scheme for the system of water layer equations (12) – (15), while the landslide is described by non-dispersive shallow water equations (16) – (17). This procedure is also implemented into the NAMI-DANCE software. The inclusion of dispersion in the water layer was carried out according to the same methodology as in Sec. 2 with the replacement of the physical dispersion by a numerical one.

This model was used to estimate the prognostic tsunami in the Nile Delta (Egypt) (Yalciner et al, 2014).

6. METEOTSUNAMI

Sometimes, large waves are generated by the sharp spatial and temporal changes in the atmospheric pressure. A low atmospheric pressure leads to an increase in the water level in the marine area part, and a high atmospheric pressure leads to a decrease in the water level of another zone ("the inverse barometer" law), so that the water level in the sea is distorted. The waves arising from it can be amplified due to the resonance properties of the coastal morphology (the Proudman and the Greenspan resonances). The observation review of the meteo-tsunami is given in (Pattiaratchi and Wijeratne, 2015). Meteorological long waves have the same wave period as conventional tsunamis (from a few minutes to 2-3 hours), they can cause human casualties and destructive effects in coastal zones, like ordinary tsunamis. For the meteorological tsunami, such generation mechanisms as spatial and temporal pressure distributions (the atmospheric fronts) and the atmospheric gravitational waves are important.

One of the widely known tsunami events of this kind was observed on June 23-27, 2014 in the Mediterranean and Black Seas from Spain to Ukraine (Sepic et al, 2015). In particular, on June 27, 2014, 1-2m high waves suddenly came to Odessa coast. Since significant earthquakes in the

Mediterranean and Black Sea regions were not recorded during these events, the atmospheric disturbances are assumed to be a possible cause.

The equations of the long-wave model now include atmospheric effects; in particular, equations (1) – (2) are modified

$$\frac{\partial M}{\partial t}+\frac{1}{R\cos\theta}\frac{\partial}{\partial\lambda}\left(\frac{M^2}{D}\right)+\frac{1}{R\cos\theta}\frac{\partial}{\partial\theta}\left(\frac{MN\cos\theta}{D}\right)+\frac{gD}{R\cos\theta}\frac{\partial}{\partial\lambda}+$$
$$+\frac{gn^2}{D^{7/3}}M\sqrt{M^2+N^2}+\frac{D}{\rho}\frac{1}{R\cos\theta}\frac{\partial p_{atm}}{\partial\lambda}=fN, \quad (19)$$

$$\frac{\partial N}{\partial t}+\frac{1}{R\cos\theta}\frac{\partial}{\partial\lambda}\left(\frac{MN}{D}\right)+\frac{1}{R\cos\theta}\frac{\partial}{\partial\theta}\left(\frac{N^2\cos\theta}{D}\right)+\frac{gD}{R}\frac{\partial}{\partial\theta}+$$
$$+\frac{gn^2}{D^{7/3}}N\sqrt{M^2+N^2}+\frac{D}{\rho}\frac{1}{R\cos\theta}\frac{\partial p_{atm}}{\partial\theta}=-fM, \quad (20)$$

and equation (3) remains unchanged. Here p_{atm} is the atmospheric pressure in Pascals, which is taken from meteorological maps, usually transmitted with an interval of one hour. Pressure distribution charts with an interval of 6 hours are available on the NASA website [https://gemini.gsfc.nasa.gov/aplo]. For computations, these maps are interpolated in time to obtain the pressure field at each time step.

Unfortunately, in this case, tsunami events are actually missing when a sharp change in the atmospheric pressure occurs in the given place within a short period of time, it just leads to the meteorological tsunami generation. Therefore, it is rather difficult to obtain the agreement with the observed data, especially if there are no more frequent observations in coastal locations. A strong amplification of meteorological tsunamis occurs at resonance, when the velocity of the atmospheric front is close to the long wave celery in the basin (the Proudman resonance) and such effects are noted in a number of regions of the World Ocean.

The NAMI-DANCE software modification with the atmospheric pressure inclusion in it is not difficult (the equation order does not change), with the exception of technical problems associated with the atmospheric maps described above. This modification has also passed verification on the well-known theoretical solutions of the linear theory of shallow water in basins with an idealized bathymetry (Metin et al, 2017).

7. TSUNAMI WAVE IMPACT ON COASTS AND STRUCTURES

The computations of wave characteristics (the water surface displacement and flow velocity) are now routine actions in tsunami modeling. The computation of tsunami force characteristics is only beginning. In the practice of wind waves loads, these characteristics are computed at the second stage, when the wave regime in the sea is known and it can be easily recounted to any point in the harbor. This way of work is not acceptable for a tsunami. Tsunami waves are long waves, the scale of which is comparable

to the size of coastal structures (harbors and ports), so it is impossible to recalculate the wave field from the open sea to the design area of construction using simple formulas in the framework of the ray tracing method.

Therefore, the design of large objects (port, dam, etc) in the coastal zone should always be accompanied by the wave regime modeling taking into account the planned structures, since the resonant properties of the water areas and the locations of the wave extrema change. Only for relatively simple small-scale structures, it is possible to carry out wave field computations independently of the planned structures, and then calculate the load on them separately. Such situation, in particular, is realized in the case of single vertical piles of a small diameter (compared to the tsunami wavelength). In some cases, the pile diameter is so small that it is "subgrid" in numerical meshes, and the perturbation inserted by the object practically does not affect the wave field. In such cases, the classical formulas for forces and moments can be used. In particular, the pressure and drag forces are

$$F_h = \frac{1}{2}\,\rho_w g D S, \qquad F_f = \frac{1}{2}\,\rho_w C_D u^2 S \tag{21}$$

(ρ_w is the sea water density and S is the cross-sectional area of the structure against the direction of the wave propagation). It can be seen that they are proportional to the kinematic characteristics of the tsunami waves (the water displacement and the flow velocity), and all construction characteristics (the pile diameter, the wall width) determine only the numerical coefficients in (21). Therefore, the calculation of the tsunami impact on the small diameter objects can be performed only after the wave field analysis in the water area is fulfilled.

The calculation of changes in the seabed and coasts is more complicated, therefore, it requires using three-dimensional transport models. Meanwhile, the sediment transport can be roughly characterized by the Rouse number (Julien, 1995). It is a non-dimensional number in fluid dynamics used to define a concentration profile of suspended sediment and which also determines how the sediment will be transported in a flowing fluid. Mathematically, it is the ratio between the sediment fall velocity W_s and the upwards velocity on the grain as product of the von Karmán constant $k$and the shear velocity u^*

$$R_0 = \frac{W_s}{\beta\kappa u^*}, \tag{22}$$

where β is the ratio of vortex viscosity to vortex diffusion. The value of the particle fall rate W_s depends on their size and density, and is constant for each sediment type. The shear velocity can be roughly related to the water flow velocity $u^* \sim u$, so that the Rouse number is inversely proportional to the water flow velocity. It is generally accepted that the sediment movement initiation occurs at Rouse numbers of about 7, and the bed-load movement occurs in the range 2.5 – 7.5. The movement of the suspended sediments corresponds to the Rouse numbers 0.8 – 1.2. At lower values of the Rouse number, a strong movement of the bottom sediments occurs, leading to significant bottom deformations. By calculating

the water flow velocity and determining the Rouse number, we can determine the character of the bottom processes. For areas of intensive changes in the bottom morphology, we can then perform a separate simulation of the quantitative characteristics of the sediment transport using various transport models.

We would like to note also the estimates of the possible house and various construction destruction on the shore produced by tsunami waves. For many areas, when the character of the buildings are taken into account, the so-called fragility curves are given that relate the percentage of damage or the relative number of deaths to the tsunami height on the coast (Nanayakkara and Dias, 2016). Such curves are determined for some areas of Japan, Indonesia, Egypt and the United States.

The calculation of all the parameters listed above is easily inserted into any computer model, and in particular, it has already been done in our NAMI-DANCE software (Ozer et al, 2015a,b; Kian et al, 2016). Let us note here that since 2018 in Russia the Code of Rules No. 292.1325800.2017 “Buildings and constructions in tsunami-hazardous areas. Design Rules”, approved on June 23, 2017 by the Ministry of Construction and Housing and Communal Services of the Russian Federation has been used.

8. CONCLUSION

This brief review provides the hydrodynamic models used in the tsunami problem which are solved with the help of the NAMI-DANCE software. They are based on the well-known two-dimensional equations of the shallow water theory, adapted to the rotating Earth, the available bathymetry database and the land topography. The numerical model takes into account the basic mechanisms of tsunami wave generation and dissipation. In some cases, it is necessary to take into account the water wave dispersion leading to the increase in the order of differential equations. In our computations, the physical dispersion is replaced by a numerical one, which allowed us not to increase the computation time significantly. The developed NAMI-DANCE software is actively used to simulate real events, prognostic tsunamis, inundation maps and tsunami force characteristics.

ACKNOWLEDGEMENTS

This study was initiated in the framework of the state task program in the sphere of scientific activity of the Ministry of Science and Higher Education of the Russian Federation (project No. 5.4568.2017/6.7 and 5.5176.2017/8.9) and financially supported by this program, the grant of the President of the Russian Federation for state support of leading scientific schools of the Russian Federation NSh-2685.2018.5 and grants RFBR (18-05-80019). EC project ASTARTE-Assessment, Strategy And Risk Reduction for Tsunamis in Europe—FP7-ENV2013 6.4-3, Grant 603839, UDAP-Ç-12-14 project granted by Disaster Emergency Management Presidency of Turkey (AFAD) and TUBITAK 113M556, 108Y227 and 213M534 Projects are also acknowledged.

REFERENCES

1. Aytore, B., Yalciner, A.C., Zaytsev, A., Cankaya, Z.C., and Suzen, M.L. Assessment of tsunami resilience of Haydrapasa port in the Sea of Marmara by high-resolution numerical modeling. Earth, Planets and Space, 2016, vol. 68, 139-150.

2. Beisel, S.A., Khakimzyanov, G.S., and Chubarov, L.B. Simulation of surface waves generated by an underwater landslide moving along a spatially irregular slope. Computational Technologies, 2010, vol. 15, 39-51.

3. Cheung, K.F., Phadke, A.C., Wei, Y., Rojas, R., Douyere, Y.J.-M., Martino, C.D., Houston, S.H., Liu, P.L.-F., Lynett, P.J., Dodd, N., Liao, S., and Nakazaki, E. Modeling of storm-induced coastal flooding for emergency management. Ocean Engineering, 2003, vol. 30, 1353-1386.

4. Choi, B.H., Kaistrenko, V., Kim, K.O., Min, B.I., and Pelinovsky, E. Rapid forecasting of tsunami runup heights from 2D numerical simulation data. Natural Hazards and Earth System Sciences, 2011, vol. 11, No. 3, 707-714.

5. Choi, J.W., Kwon, K.K., and Yoon, S.B. Tsunami inundation simulation of a built-up area using equivalent resistance coefficient. Coastal Engineering Journal, 2012, vol. 54, 1250015-1-25.

6. Dilmen, D.I., Kemec, S., Yalciner, A.C., Düzgün, S., and Zaytsev, A. Development of a tsunami inundation map in detecting tsunami risk in Gulf of Fethiye, Turkey. Pure and Applied Geophysics, 2015, vol. 172, 921-929.

7. Fedotova, Z.I., Khakimzyanov, G.S., and Gusev, O.I. History of the development and analysis of numerical methods for solving nonlinear dispersive equations of hydrodynamics. I. One-dimensional models problems. Computational Technologies, 2015, vol. 20, 120-156.

8. Garagash, I.A., Lobkovsky, L.I., Kozyrev, O.R., and Mazova, R.Kh. Generation and runup of tsunami waves at an submarine landslide. Oceanology, 2003, vol. 43, 173-181.

9. Giachetti, T., Paris, R., Kelfoun, K., and Ontowirjo, B. Tsunami hazard related to a flank collapse of Anak Krakatau Volcano, Sunda Strait, Indonesia. Geological Society, London, Special Publications, 2012, vol. 361, 79-90.

10. Glimsdal, S., Pedersen, G.K., Harbitz, C.B., and Lovholt, F. Dispersion of tsunamis: does it really matter? Natural Hazards and Earth System Sciences, 2013, vol. 13, 1507-1526.

11. Goto, C., Ogawa, Y., Shuto, N., and Imamura, F. IUGG/IOC TIME Project: Numerical Method of Tsunami Simulation with the Leap-Frog Scheme. Manuals and Guides. Paris, Intergovernmental Oceanographic Commission of UNESCO, 1997. No.35. 126 p.

12. Ivanova, A.A., Kulikov, E.A., and Fain, I.V. On modelling 2006, 2007 Simushir tsunamis in the central Kuril region. Fundamentalnaya i Prikladnaya Gidrofizika, 2017, vol. 10, 56-64 [in Russian].

13. Imamura, F., and Imteaz, M.A. Long waves in two layer: governing equations and numerical model. Science of Tsunami Hazards, 1995, vol. 13, No. 1, 3-24.

14. Julien. P.Y. Erosion and Sedimentation, Cambridge University Press, Cambridge, 1995.

15. Khakimzyanov, G., Dutykh, D., Fedotova, Z., and Mitsotakis, D. Dispersive shallow water wave modelling. Pt I: Model derivation on a globally flat space. Communications in Computational Physics, 2018, vol. 23, 1-29.

16. Kian, R., Horrillo, J., Zaytsev, A., and Yalciner, A.C. Capturing physical dispersion using a nonlinear shallow water model. Journal of Marine Science and Engineering, 2018, vol. 6, 84-1-11

17. Kian, R., Velioglu, D., Yalciner, A.C., and Zaytsev, A. Effects of harbor shape on the induced sedimentation; L-type basin. J Marine Science and Eng., 2016, No. 4, 55-65.

18. Kirby, J.T., Shi, F., Tehranirad, B., Harris, J.C., and Grilli, S.T. Dispersive tsunami waves in the ocean: Model equations and sensitivity to dispersion and Coriolis effects. Ocean Modelling, 2013, vol. 62, 39-55.

19. Kirby, J.T., Wei, G., Chen, Q., Kennedy, A.B., and Dalrymple, R.A. FUNWAVE 1.0. Fully Nonlinear Boussinesq Wave Model. Documentation and User's manual. Research Report No. CACR-98-06, Univ. of Delaware. 1998. 80 p.

20. Kostenko, I.S., Zaytsev, A.I., Minaev, D.D., Kurkin, A.A., Pelinovsky, E.N., and Oshmarina, O.E. The Moneron Tsunami of September 5, 1971, and its manifestation on the Sakhalin island coast: numerical simulation results. Izvestiya - Atmospheric and Ocean Physics, 2018, vol. 54, 1-9.

21. Kulikov, E.A., Gusiakov, V.K., Ivanova, A.A., and Baranov, B.V. Numerical tsunami modeling and the bottom relief. Moscow University Physics Bulletin, 2016, vol. 71, 527-536.

22. Kulikov, E.A., Rabinovich, A.B., Fain, I.V., Bornhold, B.D., and Thomson, R.E. Tsunami generation by landslides at the Pacific coast of North America and the role of tides. Oceanology, 1998, vol. 38, 323-328.

23. Levin, B., and Nosov, M. Physics of Tsunamis. Springer, 2009.

24. Lobkovsky, L.I., Mazova, R.Kh., Garagash, I.A., Kataeva, L.Yu., and Nardin, I. To analysis of source mechanism of the 26 December 2004 Indian Ocean tsunami. Russ. J. Earth Sci., 2006, vol. 8, ES5001.

25. Lovholt, F, and Pedersen, G. Instabilities of Boussinesq models in nonuniform depth. International Journal for Numerical Methods in Fluids, 2009, vol. 61, 606-637.

26. Lynett, P.J., Montoya, L., Gately, K., Wilson, R., Arcas, D., Aytore, B., Dogan, G.G., Kian, R., Velioglu, D., Yalçıner, A.C., Bai, Y., Cheung, K.F., Heitmann, T.W., Bricker, J.D., Roeber, V., Castro, M.J., Escalante, C., Macías, J., Yamazaki, Y, David, C.G., Gonzalez-Vida, J.M., Grilli, S.T., Shelby, S., Horrillo, J., Pampell-Manis, A., Kanoglu, U., Sharghivand, N., Kirby, J.T., Shi, F., Tehranirad, B., Li, W., Thio, H.K., Nicolsky, D.J., Ortega, S., Park, Y.S., Tolkova, E., Zaytsev, A., and Zhang, Y.J. Inter-model analysis of tsunami-induced coastal currents. Ocean Modelling, 2017, vol. 114, 14-32.

27. Madsen, P., Bingham, H.B., and Schaffer, H.A. Boussinesq-type formulations for fully nonlinear and extremely dispersive water waves: derivation and analysis. Proc. R. Soc. Lond. A, 2003, vol. 459, 1075-1104.

28. Makhinov, A.N., Kim, V.I., Ostroukhov, A.V., and Matveenko, D.V. Large landslide in the valley of the Bureya River and tsunami in the reservoir of the Bureya hydroelectric power station. Vestnik of the Far East Branch of the Russian Academy of Sciences, 2019, no. 2, 35-44 [in Russian].

29. Metin, D., Pelinovsky, E., Yalciner, A., Zaytsev, A., Tarakcioglu, O.G., Yalciner, B., Kurkin, A. meteotsunami: generation, propagation and amplification. Proc. Thirteenth Int. Conference on the Mediterranean Coastal Environment, MEDCOAST 17, 2017, vol. 2, 1143-1154.

30. Mirchina, N.R., and Pelinovsky, E.N. Nonlinear and dispersive effects for tsunami waves in the open ocean. Int. J. Tsunami Soc., 1982, vol. 2, no. 4, D1 - D9.

31. Nanayakkara, K.I.U., and Dias, W.P.S. Fragility curves for structures under tsunami loading. Natural Hazards, 2016, vol. 80, 471-486.

32. Nosov, M.A. Applicability of long-wave approximation to the description of tsunami dynamics. Moscow University Physics Scientific Notes, 2017, no. 4, 1740503-1-7 [in Russian].

33. Okada, Y. Surface deformation due to shear and tensile faults in a half-space. Bulletin of the Seismological Society of America. 1985, vol. 75, 1135-1154.

34. Omira, R., Dogan, G.G., Hidayat, R., Husrin, S., Prasetya, G., Annunziato, A., Proietti, C., Probst, P., Paparo, M.A., Wronna, M., Zaytsev, A., Pronin, P., Giniyatullin, A., Putra, P.S., Hartanto, D., Ginanjar, G., Kongko, W., Pelinovsky, E., and Yalciner, A.C. The September 28th, 2018, tsunami in Palu-Sulawesi, Indonesia: A post-event field survey. Pure and Applied Geophysics, 2019, vol. 176, 1379-1395.

35. Ozer, S.C., Yalciner, A.C., and Zaytsev, A. Investigation of tsunami hydrodynamic parameters in inundation zones with different structural layouts. Pure and Applied Geophysics, 2015a, vol. 172, 931-952.

36. Ozer, S.C., Yalciner, A.C., Zaytsev, A., Suppasri, A., Imamura, F. Investigation of hydrodynamic parameters and the effects of breakwaters during the 2011 Great East Japan Tsunami in Kamaishi Bay. Pure and Applied Geophysics, 2015b, vol. 172, 3473-3491.

37. Pattiaratchi, C.B., and Wijeratne, E.M.S. Are meteotsunamis an underrated hazard? Phil. Trans. R. Soc. A, 2015, vol. 373, 20140377-1-23.

38. Pelinovsky, E.N. Hydrodynamics of tsunami waves. Nizhny Novgorod, 1996 [in Russian].

39. Pelinovsky, E.N. Nonlinear – dispersive theory of tsunami waves: outlook after the hazardous Indian Ocean tsunami. Nonlinear waves' 2006. Nizhny Novgorod, 2007, 393-407 [in Russian].

40. Pelinovsky, E., and Poplavsky, A. Simplified model of tsunami generation by submarine landslides. Phys. Chem. Earth, 1997, vol. 21, no. 1/2, 13-17.

41. Peregrine, D.H. Long waves on a beach. J. Fluid Mechanics, 1967, vol. 27, 815-882.

42. Pudasaini, S.P., and Hutter, K. Avalanche Dynamics: Dynamics of Rapid Flows of Dense Granular Avalanches. – Springer, 2006.

43. Sassa, Sh., and Takagawa, T. Liquefied gravity flow-induced tsunami: first evidence and comparison from the 2018 Indonesia Sulawesi earthquake and tsunami disasters. Landslides, 2019, vol. 16, 195-200.

44. Sepic, J., Vilibic, I., Rabinovich, A.B., and Monserrat, S. Widespread tsunami-like waves of 23-27 June in the Mediterranean and Black Seas generated by high-altitude atmospheric forcing. Scientific reports, 2015, vol. 5, 11682-1-8.

45. Science Global News, 2018. http://scienceglobalnews.com/environment/meteotsunami-floods-islands-of-mallorca-and-menorca-spain (accessed 28 March 2019).

46. Shokin, Yu.I., Fedotova, Z.I., and Khakimzyanov, G.S. Hierarchy of nonlinear models of the hydrodynamics of long surface waves. Doklady Physics, 2015, vol. 60, No. 5, 224-228.

47. Sogut, D.V., and Yalciner, A.C. Performance Comparison of NAMI DANCE and FLOW-3D models in tsunami propagation, inundation and currents using NTHMP benchmark problems. Pure Appl. Geophys., 2019, vol. 176, 3115–3153

48. Tufekci, D., Suzen, M.L., Yalciner, A.C., and Zaytsev, A. Revised MeTHuVA method for assessment of tsunami human vulnerability of Bakirkoy district, Istanbul. Natural Hazards, 2018, vol. 90, 943-974.

49. Velioglu, D. Kian, R., Yalciner, A.C., and Zaytsev, A. Performance assessment of NAMI DANCE in tsunami evolution and currents using a benchmark problem. Journal of Marine Science and Engineering, 2016, vol. 4, 49-1-8.

50. Wells, D.L., and Coppersmith, K.J. New empirical relationships among magnitude, rupture length, rupture width, rupture area, and surface displacement, Bull. Seism. Soc. America, 1994, vol. 84, 974-1002.

51. Yalciner, A.C., Pelinovsky, E.N., Okal, E, and Synolakis, C.E. (Eds) Submarine landslides and tsunamis. Kluwer, 2003.

52. Yalciner, A.C., Zaytsev, A., Aytore, B., Insel, I., Heidarzadeh, M., Kian, R., Imamura, F. A possible submarine landslide and associated tsunami at the northwest Nile Delta, Mediterranean Sea. Oceanography, 2014, vol. 27, 68-75.

53. Yoon, S.B. Propagation of distant tsunamis over slowly varying topography. J Geophysical Research, 2002, vol. 107, no. C10, 4-1- 4-11.

54. Yoon, S.B., Lim, C.H., and Choi, J. Dispersion-correction finite difference model for simulation of transoceanic tsunamis. Terrestrial Atmospheric and Oceanic Sciences, 2007, vol. 18, 31-53.

55. Zaytsev, A., Kostenko, I., Kurkin, A., Pelinovsky, E., Pararas-Carayannis, G. Manifestation of the 1963 Urup tsunami on Sakhalin: observations and modeling. Science of Tsunami Hazards, 2017, vol. 36, 145-166.